Journal of Applied Polymer Science

Ag-nanocomposite based on carboxymethylcellulose for humidity detection: Green synthesis and sensing performances

Wiem Marzouk,[1] Nawfel Sakly,[1,2] Sadok Roudesli,[1] Hafedh Ben Ouada,[1,2] Hatem Majdoub[1]

[1]Laboratory of Interfaces and Advanced Materials, Faculty of Sciences of Monastir, University of Monastir, Avenue De L'environnement, Monastir 5019, Tunisia

[2]Higher Institut of Applied Sciences and Technology of Mahdia, University of Monastir, Mahdia, Sidi-Messaoud 5011, Tunisia

Correspondence to: H. Majdoub (E-mail: hatemmajdoub.fsm@gmail.com)

ABSTRACT: A novel highly sensitive Ag-nanocomposite for humidity detection has been successfully prepared. Initially, cellulose isolated from Tunisian palm date petiole was converted to carboxymethyl cellulose (CMC) as biomatrix under heterogeneous conditions. The synthesized product was thoroughly characterized by means of FT-IR spectroscopy, viscosity analysis, and high performance size exclusion chromatography multiangle laser light scattering. CMC was used as reducing and stabilizing agent to prepare CMC-stabilized silver nanoparticles via a rapid green method. The bioreduction of silver ions under different experimental conditions, including Ag^+ concentration and pH, was investigated. Optimal experimental conditions provided a long-term stable colloidal suspension and well-dispersed spherical shape Ag NPs with a size ranging from 13 to 28 nm. Ag-nanocomposite coated quartz microbalance crystal was used as sensitive layer for humidity detection. A comparative study showed that the immobilized metallic nanostructures greatly reduced changes in visco-elastic properties, increased surface area as well as surface local charge density of the CMC. Consequently, sensor performances were greatly enhanced: better stability even at higher relative humidity (RH), good reproducibility and linearity (11–98% RH), low hysteresis characteristics, and rapid response and recovery times (14 and 6 s, respectively) were obtained. © 2016 Wiley Periodicals, Inc. J. Appl. Polym. Sci. **2016**, *133*, 43686.

KEYWORDS: cellulose and other wood products; composites; nanoparticles; nanowires and nanocrystals; properties and characterization; sensors and actuators

Received 29 December 2015; accepted 22 March 2016

DOI: 10.1002/app.43686

INTRODUCTION

Humidity measurements are important in various fields, including environmental (i.e., human comfort and weather forecast), industrial, agricultural, clinical, biotechnological and food conservation domains.[1] Therefore, the requirement for low cost and reliable humisensors is essential. The moisture signal response can be followed by various transduction methods (i.e., optical, capacitive, resistive, and gravimetric) as previously reported.[2] Microacoustic sensors, including surface acoustic waves (SAW) and quartz crystal microbalance (QCM) sensors, are extensively used as a sensitive platform in gravimetric transduction. Typically, QCM sensors are more practical due to their small size, cost-effective, low power consumption, high stability, and high resolution mass variation on the nanogram scale.[3] Consequently, the online humidity detection can be achieved by following the shift of the crystal resonance frequency directly related to the adsorbed mass of water molecules on a rigid surface attached to the QCM according to the Sauerbrey equation[4] given by:

$$\Delta F = -2.26\ 10^6\ f_0^2\ \Delta m/A \quad (1)$$

where ΔF (Hz) is the measured frequency shift, f_0 (MHz) is the fundamental frequency of the unloaded QCM, A (cm^2) is the surface area of the electrode, and Δm (g) is the change in mass on the surface of the crystal due to the sorption of target molecules from the environment on the sensing layer.

Nevertheless, changes in viscoelastic properties of nonrigid sensitive layer marked by a positive frequency shift were previously reported, especially during exposure to high humidity levels.[5] Therefore, to separate the contribution of the competitive processes, Hunt *et al.*[6] derived a generalized equation using the time-dependent perturbation theory and the total frequency shift was given by the following expression:

$$\Delta F = \left(-2.26\ 10^6 f_0^2 \Delta m/A\right) + \left(+2.26\ 10^6 f_0^2 h_f \Delta\mu_f / V_s^2\right) \quad (2)$$

where V_s is the acoustic velocity across the deposited film thickness and h_f and μ_f are the thickness and the shear stiffness of the sensing layer, respectively. Clearly, the first term is the classical Sauerbrey equation while the second term reflects change in

viscoelastic properties of the sensing layer. Commonly, negative frequency shifts of resonance frequency have been observed for sensing materials coated as active layer on the QCM electrode for moisture detection including MWCNT,[7] graphene oxide,[8] ZnO nanostructures,[9] and polyelectrolytes.[10] Conversely, Erol *et al.*[11] benefit of the changes in the viscoelasticity as well as the mechanical stiffness ZnO cotton-structure nanowires, for humidity detection.

Although many successes are obtained, many efforts are devoted to enhance humidity sensors performances to meet the requirements of environmental and air-quality monitoring. Actually, several methods have been reported to enlarge surface hydrophilicity of the sensing layer,[12] increase its specific surface area[13,14] and modify surface reactions by doping with catalytic elements.[15] Moreover, it is found that nanocomposite sensing layer exhibits higher sensitivity, better stability, and fast response and recovery times compared to the single component.[16] More recently, metallic nanosized materials such as gold nanoparticles (Au NPs) have been used owing to their high surface area and availability of many active sites for low humidity detection.[17] According a recent literature review, there is no report about QCM coated with bionanocomposite based on silver nanoparticles (Ag NPs) for humidity detection.

In fact, Ag NPs have drawn great interests in diverse research fields including cell imaging, bacteriology, quantum information processing, optical spectroscopy, and LSPR based sensors, as previously reported.[18–21] Their synthesis according to a classical chemical reduction route using sodium borohydrique,[22] sodium citrate,[23] fructose,[24] and formamide[25] are extensively reported. Currently, green method offers a new approach for one-pot synthesis of bionanocomposites based on natural polymers[26–28] as reducing agent and stabilizer. Therefore, replacing synthetic polymers by natural ones is a new strategy for preparing biocompatible products to overcome many socioeconomic and recycling problems. Cellulose, as an important structural component of primary cell wall plants and many form of algae and bacteria, remain the most common eco-friendly raw material, biodegradable, low cost biopolymer with large abundance on earth.[29] However, the full potential of cellulose has not yet been exploited since its solubility in the common organic solvent is limited and chemical modifications are required. Mostly, carboxymethyl cellulose (CMC) is the oldest and, a renowned water soluble polyelectrolyte extensively used in pharmaceutical, detergent cosmetics, foods, and textile industries.[30–32]

The present work is undertaken within the framework of a research program in our laboratory, focused on the synthesis and the enhancement of sensing properties of sensitive layers based on natural polymers for sensor applications. This is accomplished firstly by the conversion of plant waste materials, including those from date palm (*Phoenix dactylifera* L.), into valuable water soluble polyelectrolytes as matrix for nanocomposites. The date palm was chosen instead of other cellulose sources because of its abundance and relevant role in south of Tunisia on the socioeconomic and ecological levels.

In this work, we are interested in the extraction and chemical modification of Tunisian date palm petioles fibers for CMC synthesis. The obtained product was fully characterized by means of FT-IR, SEC and viscosity analysis. Moreover, the obtained polyelectrolyte was used as reducing and stabilizing agent for green, rapid, method synthesis of CMC-stabilized Ag NPs. Sensing properties of CMC and CMC-Ag NPs nanocomposite coated over a QCM for humidity sensor were also investigated in the range of relative humidity (RH) of 0–98% RH. Several considerations were taken into account to elucidate the major causes of improved sensor performances.

EXPERIMENTAL

Chemicals

All used chemicals are analytical grade or of the highest purity available. Low viscosity carboxymethyl cellulose sodium salt (30–70 mPa for 1% solution in water at 20 °C) was purchased from VWR International and chosen as reference for comparative study. Sodium monochloroacetate ($C_2H_2ClO_2Na$), sodium chlorite ($NaClO_2$), sodium hydroxide (NaOH, >98%), isopropyl alcohol, and ethanol are purchased from Sigma-Aldrich (Tunisia). Silver nitrate ($AgNO_3$) is obtained from Panarec Quimica, S.A. (Barcelona).

Date Palm Petioles

The date palm petiole used in this study was collected from Monastir (April 2011) as shown in Figure 1(a). The sample was dried under natural conditions (at 25 °C and 60% relative humidity). Subsequently, the obtained materials were milled and sieved to produce grains between 200 μm and 1 mm

Extraction and Purification of Cellulose Fibers

The organization of the polysaccharides in the plant cell wall was essentially produced by a network of hydrogen bonds between the different polymers. Their separation can be achieved by treatments to break hydrogen bonds. The extraction under alkaline conditions was considered as the best method to remove hemicellulose, breaks the hydrogen bonds, and the hydrolyzed ester groups.[33] The different stages of extraction and purification processes were sketched in the flow chart given in Figure 1(b). Following the depigmentation process, the extraction was carried out using a sodium hydroxide solution (2M) at 80 °C during 2 h. The obtained product was subsequently bleached with sodium chlorite in an acidic medium.

Synthesis of Carboxymethyl Cellulose (CMC)

The extracted and purified cellulose from Tunisian date palm petiole was converted to carboxymethyl cellulose (CMC) in two steps including an alkalization step and an etherification of cellulose step under heterogeneous conditions. In alkalization pretreatment, cellulose fibers were immersed in 60 mL of isopropanol under vigorous stirring at room temperature. A 40% of a sodium hydroxide solution was added dropwise and stirred for an hour at 60 °C. Afterward, the mixture was left overnight under stirring at room temperature. After the alkali treatment, the etherification process was performed by adding a certain amount of sodium monochloroacetate in the reaction mixture and placed in a water bath at 55 °C for 5 h under vigorous stirring. The obtained solution was cooled and precipitated in methanol. The precipitate was filtered, redissolved in distilled water, neutralized with an acetic acid solution to adjust the pH between 6 and 8 and

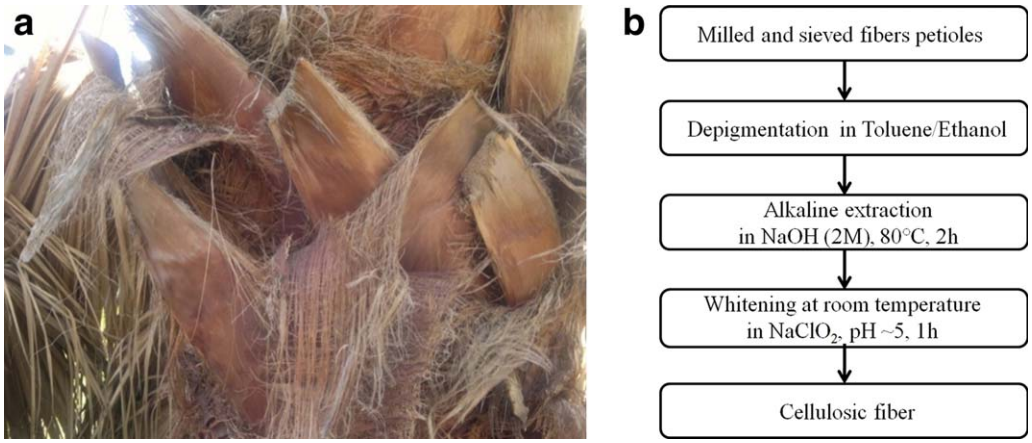

Figure 1. (a) Petiole fiber of Tunisian date palm used in this work. (b) The schematic flow chart diagram for the extraction and bleaching of cellulose fibers date palm. [Color figure can be viewed in the online issue, which is available at wileyonlinelibrary.com.]

reprecipitated in ethanol. Subsequently, the product was washed with ethanol and dried under vacuum at 40 °C. Finally, a white powder with a yield of 26.6% was obtained.

Green Synthesis of Ag-NPs

The synthesis of CMC-stabilized Ag NPs at different concentrations of silver ions (Ag^+) and various pH values at 90 °C is quite straightforward. In typical preparation, a stock aqueous solution of $AgNO_3$ (0.1M) and 0.3 wt % of CMC aqueous solution were prepared separately. First of all, different volumes of aqueous solution of silver ions [25 μL (S1), 50 μL (S2), 100 μL (S3), 250 μL (S4), 500 μL (S5), 1000 μL (S6), and 1500 μL (S7)] were injected to the CMC aqueous solutions and heated at 90 ± 2 °C. Subsequently, 0.5 ml of an aqueous NaOH solution (1M) was added under vigorous shaking. Short time after addition of the base, the reaction medium acquired different colors, varying from faint yellowish color to grayish color, as depicted in Figure 2. Furthermore, the effect of the pH of the reaction media on the bioreduction of silver ions was studied by keeping constant the silver ion volume at 250 μL and adding 0.1, 0.25, 0.5, and 1.0 mL NaOH aqueous solution.

In all experiments, bioreduction kinetic evolution of silver ions was followed at different time intervals by UV–vis spectrophotometery until the absorbance acquired a constant value. Afterward, the colloidal solutions were cooled at room temperature and finally conserved in normal laboratory conditions (NLC).

Characterization and Analysis

The ATR-FTIR spectra of cellulose and CMC were determined by infrared spectrometer PERKIN ELMER spectrum Two ATR-FTIR in the frequency range of 4000–450 cm^{-1}. Moreover, all the viscosity measurements were carried out in triplicates at room temperature. The average values were reported using a capillary viscosimeter (PHYWE Physics, Ref: 03102-00) with a capillary diameter of 1.2 and 250 mm of length. The intrinsic viscosity of the CMC product was determined using different concentrations of NaCl according the linear regression procedure of the reduced viscosity–NaCl concentration plot. For this purpose, experiments were performed in lower concentration regime, in presence of 0.5M NaCl concentration, to complete screening of carboxylate ions and validate the expansion of the Huggin series[34] expressed as follows:

$$\eta_{red} = [\eta] + K'[\eta]^2 C + \ldots \quad (3)$$

where η_{red} is the reduced viscosity, $[\eta]$ is the intrinsic viscosity, C assigns the concentration of the CMC, and K' is the Huggins coefficient.

Furthermore, the average molecular mass in number (M_n) and weight (M_w) was determined using high performance size exclusion chromatography multiangle laser light scattering (HPSEC–MALLS). The HPSEC system is equipped with a triple detection (refractometric detection, viscosity, and multiangle light scattering). It consisted of a pump type Shimadzu LC10 Ai (flow 0.5 mL/min) and two columns OHPAK SB 804 and 806 HQ. The analysis was performed from a data processing Zimm order 1 using angles from 5 to 16 (from 34.8° to 142.8°). The Astra 6 software package was set to collect and extrapolate data with the aim to obtain for each elution volume the molecular weight and the gyration radius. With an integration of the peak, we calculated the molecular mass in number (M_n) and weight (M_w) and the z-average gyration radius. The sample was dissolved in the eluent (0.1M, $LiNO_3$) at 0.5 g/L.

The degree of substitution (DS) was determined according to the titration method using the following equations[35,36]:

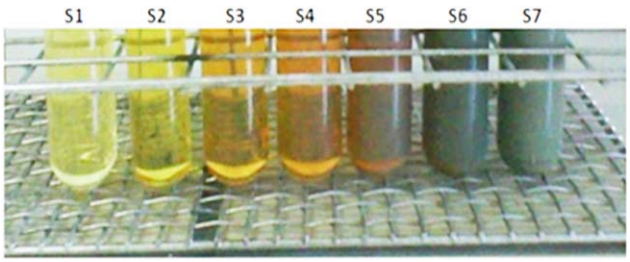

Figure 2. Digital photographs of the colloidal solutions prepared with different volumes of Ag+ 608 609 (0.1M) at 90 °C using 0.5 mL of NaOH. [Color figure can be viewed in the online issue, which is available at wileyonlinelibrary.com.]

$$B = 0.1\ V/m \quad (4)$$

$$DS = 0.162\ B/(1-0.08\ B) \quad (5)$$

where 0.1 is the sulfuric acid solution molarity, B is the titration parameter allowing the DS determination, V is the total volume consumption of acid added to neutralize the ash-based solution, m is the weight of the initial oven-dried CMC substrate, and 0.162 and 0.08 are the molar masses of the glucose units and $CH_2COO^-\ Na^+$ groups (kg mol^{-1}), respectively.

In another hand, optical properties of CMC-stabilized Ag NPs colloidal suspensions were studied using a DR5000-Hach-Lange spectrophotometer (Camlab, UK) with a variable wavelength from 200 to 1100 nm with a step of 2 nm. Particle size and morphology of Ag NPs are investigated using atomic force microscopy (AFM). The AFM observations are conducted on Scanning Probe Microscope [Digital Instruments of Dimension 3100 AFM (Veeco Metrology Group, Santa Barbara, CA)] in tapping mode using etched-silicon probe (RTESP-type, Veeco). The contrast phase image was recorded by collecting 512 × 512 points for each scan.

Apparatus, Experimental Procedure, and Sensor Configuration

Circular-shaped AT-cut polished quartz crystals with a fundamental resonance frequency of 6 MHz were obtained from INFICON. Before coating, the gold electrodes were carefully cleaned in acetone for 30 min, rinsed with methanol and subsequently blown with pure nitrogen. Afterward, bare QCM were functionalized with CMC and CMC-stabilized Ag NPs thin films produced by drop-casting method using a laboratory-made setup and dried for 48 h in normal laboratory conditions (22 °C, 56%RH).

Humidity sensing experiments were performed in a system using dynamic vapor sensing (DVS) method previously described in Ref.[37] Before determining the different performances of each functionalized QCM, a blank test was performed. The total frequency shift of the bare QCM after increasing the RH from ~0% up to 98% RH was approximately 50 Hz with a frequency drift lesser than 10 Hz within 3 h. Consequently, any frequency shift of more than 50 Hz is not assigned to the experimental fluctuations and transducer response. Next, the sensors were individually characterized according to a global sequence including stability, sensitivity, reproducibility, response, and recovery times in two different processes: humidity ascending mode (HA-mode) and humidity descending mode (HD-mode). In testing, response time (the time needed to reach 90% of the final impedance for a given RH) and recovery time (the time taken for the signal to come to within 10% of the initial value) can be accurately determined by switching the sensor between 0% RH and 98% RH in HA-mode and HD-mode, respectively, since the volume of the test-cell is small (31.25 cm^3).

RESULTS AND DISCUSSION

Characterization of the CMC Prepared from Date Palm Petiole

The carboxymethylation reaction under heterogeneous conditions was evidenced by FT-IR spectroscopy. Figure 3(a) shows the FT-IR spectra of purified cellulose and modified raw material. The chemical modification provided new characteristic absorption bands at 1615, 1425, and 1316 cm^{-1}assigned to the C═O carboxylate group(—COO^-Na^+) stretching vibration, the C—O stretching in CO_2H and —CH_2binding vibration modes, respectively.

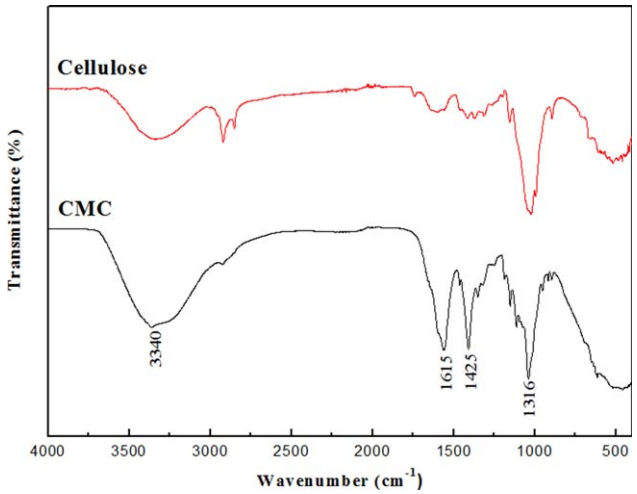

Figure 3. Infrared spectra of carboxymethylated fiber and cellulose fiber of the date palm. [Color figure can be viewed in the online issue, which is available at wileyonlinelibrary.com.]

Moreover, under heterogeneous conditions, the reaction rate is extremely sensitive to the diffusion of the reagents inside the cellulose. In this work, we use isopropyl alcohol, as solvent reaction, and a short reaction time of about 1 h.[38] The high obtained DS value (0.96) could be mainly related to the better miscibility of the etherifying reagent in isopropyl alcohol which results in a superior reactivity with the hydroxyl groups of the cellulose. Obviously, since the DS value was greater than 0.4,[39] a fully water soluble CMC was obtained.

Additionally, an average molecular number and weight of about 30,000 and 131,000 g mol^{-1}, respectively, were obtained. The average values are in agreement with the molecular weight (90,000 g mol^{-1}) of the commercially available CMC (low viscosity) previously mentioned. Nevertheless, the slight difference in M_w value is mostly attributed to the difference in cellulose source and the extraction method.

Furthermore, viscosity analysis revealed an intrinsic viscosity value of about 20.8 mL g^{-1} lower than the commercially available product ($[\eta] = 58$ mL g^{-1}) was obtained. According to these results, a random coil conformation of the synthesized CMC is expected.

Characterization of Ag NPs Prepared by Green Method

The effect of silver ions concentration, as first reaction parameter, was investigated according to a simple visual inspection of color changes of the prepared solutions using 0.5 mL of NaOH at 90 °C. The digital photograph, shown in Figure 2 evidenced the progress of the suspension color from faint yellowish (S1) to yellow-orange color (S4) as the injected volume of Ag^+ ions did not exceed 250 μL. Nevertheless, for a critical volume of 500 μL (S5), an orange-brownish color containing several black spots was observed. With a further increase in Ag^+

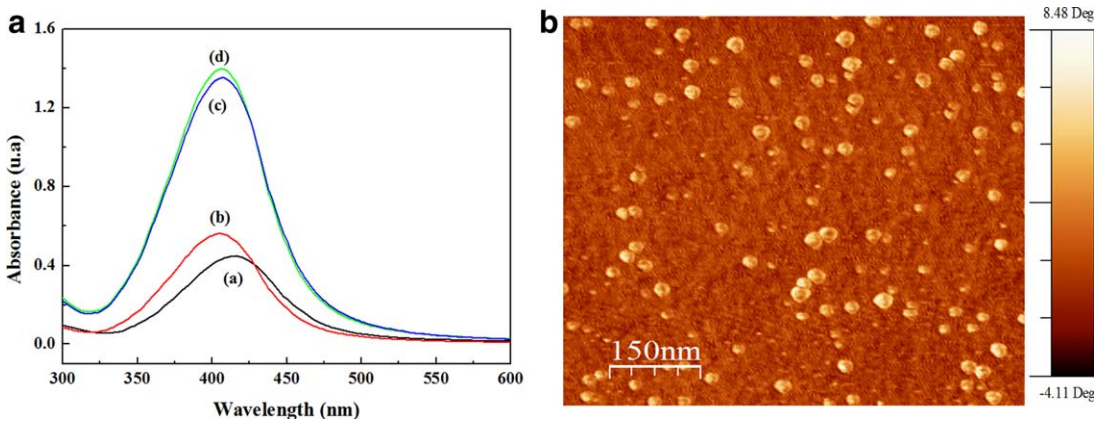

Figure 4. (a) UV–vis spectra of silver nanoparticles prepared at different volumes of NaOH (a) 0.1 mL, (b) 0.25 mL, (c) 0.5 mL, and (d) 1.0 mL at 90 °C using 250 μL of Ag+ 612 (0.1M). (b) AFM contrast phase image of the as-prepared Ag nanoparticles. [Color figure can be viewed in the online issue, which is available at wileyonlinelibrary.com.]

concentration, a grayish color and turbid solutions (S6 and S7) are clearly observed. In fact, the black spots as well as the grayish color indicates an increase from nanosized silver particles to bulk material resulted from the limitation of the CMC power stabilizing for higher concentrations of silver ions.

Furthermore, Figure 4(a) illustrates the LSPR bands evolution following variation of the pH synthesis. In fact, a broad LSPR band and low absorbance strength were observed for the lowest NaOH volume suggesting the formation of Ag NPs with different distribution sizes. As the concentration of NaOH increased from 0.1 to 0.5 mL, it was found that the absorbance strength increased, the LSPR bands became sharper, and blue shifted from 416 to 407 nm. It is important to notice that a further increase of NaOH volume (up to 1.0 mL) did not affect the optical properties of the prepared Ag NPs.

In light of the obtained results, the corresponding absorption spectrum of the optimal colloidal solution (S4) consisted in a single, symmetrical sharp and narrow LSPR band (ca. FWHM 75 nm) centered at 407 nm. Such optical properties are rather typical of spherical and quasi-mono-disperse silver nanoparticles, as previously reported.[40–42] Obviously, higher temperature and alkaline media improved the reducing power of glucose groups leading to a better reaction yield and fast nucleation process. The latter provided instantaneous color change from colorless to yellow-orange color and thereby a rapid synthesis (5 min approximatively) of spherical quasi-monodisperse nanoparticles. Such characteristics are supported by the AFM characterization as shown in Figure 4(b). In fact, the contrast-phase image revealed spherical Ag NPs with low dispersity in size since it ranged from 13 to 28 nm. Nonetheless, extending the reaction duration was clearly marked by a marginal color change from yellow-orange to grayish color, an increase in the turbidity and finally a precipitation of silver particles.

Consequently, the optimal experimental conditions including 250 μL of Ag^+ ions, 0.5 mL of NaOH as catalysis, and a temperature of 90 °C are sufficient to reduce completely silver ions and obtain a stable colloidal suspension in a short reaction time without any sign of aggregation even after 3 months of storage.

Next, possible mechanisms involved in proposed synthesis method are discussed. Previous reports[43] demonstrated that the synthesis and stabilization of Ag nanoparticles suggested different stages including complexation of silver ions, metallic atom formation and subsequently polymerization process.

Initially, a complexation process occurred between the silver ions and the extensive number of functional groups including hydroxyl and carboxyl moieties supported on the CMC. The latter exhibiting a statistical random coil conformation acted as a nano-reactor and template for nanoparticles growth. Really, bioreduction of complexed Ag^+ ions arised by the available glucose groups of the CMC in alkaline pH and at relatively high temperature (90 °C). Hence, the produced silver atoms operated as nucleation centers and the complete bioreduction was performed according to the autocatalytic reduction process. Interestingly, in addition to its reducing effect under the optimized experimental conditions, the glucose groups were oxidized to gluconic acid and an electrostatic stabilization process was expected. Really, the repulsion between the negative charges, including the initial carboxylic acid and gluconic acid groups surrounding the Ag NPs prevented their coalescence. However, taking into account the high molecular weight of the synthesized CMC, a steric stabilization process should be considered. Surely, an insufficient concentration of biopolymer cannot restrict the nanoparticle size and further growth of uncapped Ag NPs leaded to uncontrollable coalescence and aggregation of nanometals to bulk silver material.

Humidity Sensing Properties

In this section, the benefit of using the optimized CMC-stabilized Ag NPs rather than the pure CMC as sensitive layer for humidity detection was demonstrated. For this purpose, sensor characteristics of the prepared QCM sensors were examined and gathered in Table I. For comparison, Table II summarizes sensor performances of the optimized humisensor as well as several previously developed gravimetric humidity sensors exhibiting nonlinear calibration curves.

Figure 5(a) displays the variations in frequency shift in HA-mode and HD-mode of CMC and nanocomposite thin films at

Table I. Sensor Performances of the CMC and the CMC-Stabilized Ag NPs Coated QCM Sensor

	CMC	CMC-stabilized Ag NPs
Linear fitting equation	Y 1.88815 + 0.01723 X	$Y = 2.15283 + 0.01511$ X
Correlation coefficient (R^2)	0.98010	0.9963
Linearity range (% RH)	11–75	11–98
Hysteresis (%)	18	3
Long-term stability (days)	—-	>200
Response time (s)	******	14
Recovery time (s)	******	6

(—-): instability of measurements.
(******): not estimated value.

different RH levels. Obviously, the behaviors of the sensitive layers against moisture are entirely different especially above 75%RH. Really, it was observed that as %RH increased, the frequency shift of pure biopolymer modified QCM decreased slowly up to 40%RH and more sharply at 75%RH. However, further humidification until 98%RH caused a drastic positive frequency shift. Conversely, the nanocomposite loaded on QCM crystal exhibited a gradual decrease in frequency shift in the whole investigated range of RH frequently observed in humidity sensor technology based on gravimetric transduction.[10,14]

Afterward, hysteresis characteristic, which should be small as possible for humidity detection application, was evaluated. Unfortunately, the CMC thin film shows an obvious hysteresis loop in the whole range of RH estimated to be around 18% against 3% for the nanocomposite sensing layer. Additionally, it can be seen in the same figure that the frequency shifts as a function of the RH did not show a linear tendency with increasing RH regardless the sensitive layer. Similar behavior was previously observed for ZnO QDs,[37] bacterial cellulose[10] as well as fibrous composite polyacrylic acid (PAA)/poly(vinyl alcohol) (PVA) membranes[14] coated QCM humidity sensors. Commonly, the deviation from linearity of the calibration curve was widely interpreted according to multi-molecular adsorption models including BET adsorption theory.[44] Under these circumstances, the linearization of the responses was conducted in semilogarithmic plot ($\log_{10}(-\Delta F)$ versus RH) as sketched in Figure 5(b). The data in Table I derived from Figure 5(b) was computed by linear fitting. The linearity was defined as the square of correlation coefficient value (R^2) of linear fitting curve and the sensitivity as the slope of the linear regression equation. Clearly, the nanocomposite functionalized QCM transducer exhibited better linearity and larger humidity range detection compared to the CMC coated QCM sensor. Nevertheless a slight decreasing in sensitivity following immobilization of Ag nanoparticles was detected. Overall, such performance remained larger than that obtained for pure ZnO QDs sensitive layer reported in our previous study[37] and comparable to that estimated for organic coating.[10,14]

Long-term stability of the CMC and CMC-stabilized Ag NPs coated QCM sensor was also investigated. For this purpose, the measurements were repeated at room temperature every week for 4 months, followed by measuring frequency between 11% and 98%RH. For better clarity, the frequency shift curves with time at various RH are presented separately as shown in Figure 6(a) and 6(b). In opposition to the pure CMC thin film, better long-term stability of the nanocomposite in the whole humidity range was observed.

Then, considering the preliminary different study factors, the QCM coated with CMC-stabilized Ag NPs sensing layer was chosen as the most appropriate gravimetric sensor for moisture detection application.

Besides, the typical time-dependency of the optimized sensor measured for the first humidity cycle, including the HA-mode

Table II. A Comparison between Sensor Performances of the Developed Nanocomposite Coated QCM Sensor and Several Gravimetric Humidity Sensors Previously Reported in Literature

	Sensitivity	Linearity	Response time (s)	Recovery time (s)	Linear range (%RH)	Hysteresis (%)
CMC-stabilized Ag NPs	0.01723	0.9963	14	6	11–98	3
ZnO (8 nm)[37]	0.00909	0.99521	17	11	22–98	6
ZnO (100 nm)[44]	0.01884	0.99760	65	15	33–98	*****
Nanofibrous bacterial cellulose membrane[10]	0.02265	0.9980	89	*****	20–98	*****
Fibrous PAA/PVA membranes[14]	0.02093	0.97295	95	*****	20–95	*****

(*****): not reported value.

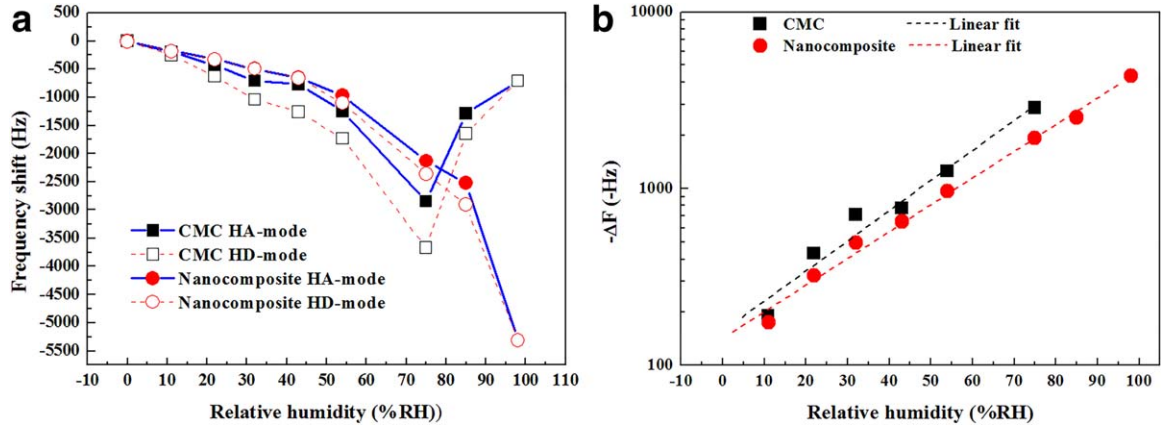

Figure 5. (a) Frequency shifts of QCM humidity sensors coated with CMC and CMC-Ag NPs 615 composite layers measured in HA- mode and HD-mode. (b) Calibration curves in semilogarithmic scale obtained from (a). [Color figure can be viewed in the online issue, which is available at wileyonlinelibrary.com.]

and HD-mode, ranging from 0%RH to 98%RH is shown in Figure 7. In the same figure, the frequency shifts response curves obtained following a repetitive rapid switching from 0 to 98%RH was also displayed. The kinetic study revealed that the frequency shift recovered to the original value following several cycles of adsorption–desorption indicating that the CMC-stabilized Ag NPs sensing layer has good frequency reproducibility. Subsequently, we determined the response and recovery times according to the method previously described in this paper. The estimated average response and recovery times were 14 and 6 s, respectively, which are shorter than those obtained for the earlier developed humisensor based on QCM coated with 8[37] and 100 nm[44] average diameter ZnO nanoparticles.

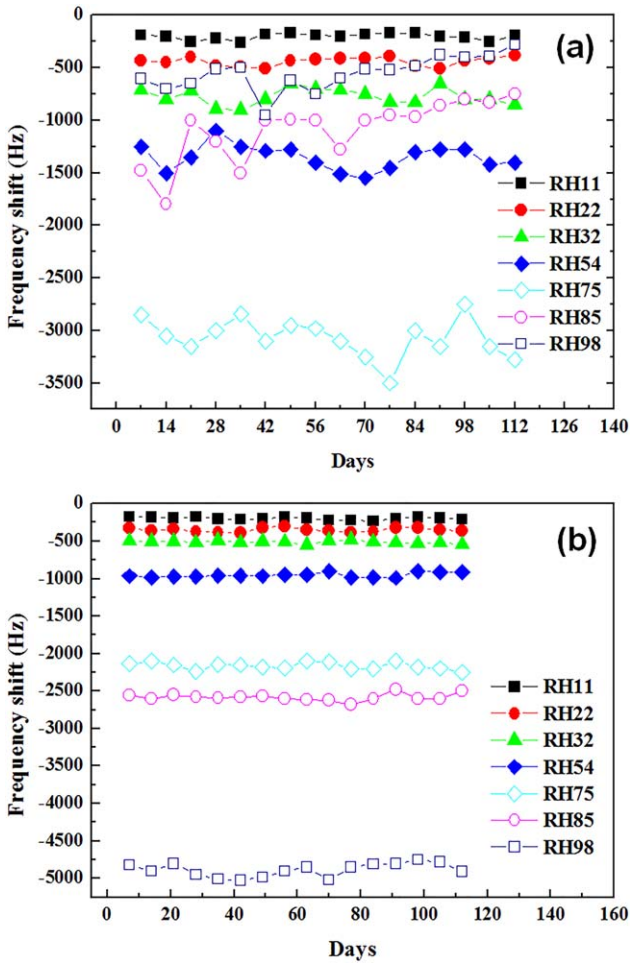

Figure 6. Frequency shift with time at various RH levels: (a) CMC, (b) nanocomposite coated QCM sensor. [Color figure can be viewed in the online issue, which is available at wileyonlinelibrary.com.]

Sensing Mechanisms

Herein, the major causes of sensor performances improvement were highlighted. In this aim, we based our explanation on the change in surface morphology, mechanical and surface chemistry properties following immobilization of Ag NPs in the biopolymer.

Typically, the highly sensitivity of the water soluble CMC coated QCM sensor toward moisture could be ascribed to the abundance of adsorption sites including carboxyl moieties and hydroxyl supported on polymer backbone. Formerly, it was proved that ZnO

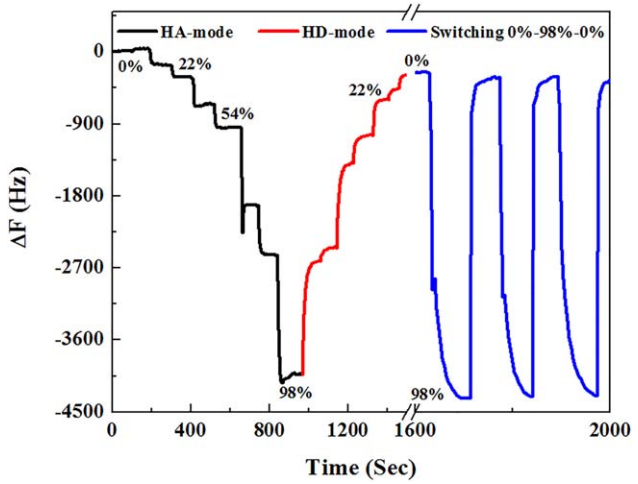

Figure 7. Time-dependent frequency shifts of the QCM coated with CMC-Ag NPs composite 618 (a) HA-mode (b) HD-mode, and (c) rapid switching between 0 and 98%RH. [Color figure can be viewed in the online issue, which is available at wileyonlinelibrary.com.]

QDs humidity sensitive layer[37] exhibited a hysteresis effect (around 6%) occurring at high RH due to the water molecules trapped in the porosity. According to Kelvin's law, the smaller is the pore radius; the lower is the RH value at which capillary condensation begins.[45] Hence, the obvious hysteresis characteristic observed in the whole of range of RH for the CMC thin film is firmly related to its cotton-like structure promoting capillary condensation process even at low RH.

Undoubtedly, higher the Flory–Huggins interaction parameter (χ_{12}) is, better affinity to solvent and swelling of polymer are. Truly, the flexibility of the polymeric chains as well the porosity enhanced the swelling of the hydrophilic thin layer and water diffusion. So changes in mechanical properties of the sensing layer are expected. Actually, the positive frequency shift detected above 75% RH arises from changes in viscoelasticity of the deposited layer. Such trend was deeply studied by Hunt *et al.*[6] using the time-dependent perturbation theory and previously reported by Erol *et al.*[11] and Horzum *et al.*[13] to explain the poor adhesion and changes in the mechanical stiffness of the porous ZnO film on the QCM electrode in moisture. Considering these issues, it seems that the noncovalent interaction between the highly water soluble CMC and the gold electrode and the swelling effect remained the major reasons of the poor adhesion of the deposited layer and the instability of the sensor response and thereby its limited lifetime.

Yet, except sensitivity, the long-term stability, reproducibility and hysteresis performances were greatly improved when the optimized CMC-stabilized Ag NPs were used as humidity sensitive layer. It is well established that the inorganic filler enhance significantly the stiffness of the nanocomposite. Therefore, the well dispersed and stabilized Ag nanoparticles, clearly shown in AFM image, raised the rigidity of the nanocomposite thin film. Consequently, the swelling as well as hysteresis effect was conspicuously reduced whereas the reproducibility and long-term stability were strikingly enhanced. Under these circumstances, the positive frequency shift contribution in the Hunt equation (2) could be neglected in the whole range of RH allowing describing the response of the nanocomposite coated QCM sensor according to the classical Sauerbrey equation for rigid coating.

Alternatively, metallic nanostructures increased significantly the surface roughness as well as the local surface charge density of the humidity sensitive layer. As a result more surfaces available for moisture uptake, better dissociation of adsorbed water and highest binding affinity are expected. Nevertheless, the unpredictably slight drop in sensitivity is probably attributed to the decrease of the hydrophilic functional groups which were involved to stabilize the nanometals. Further studies are underway to optimize the Ag NPs content in the nanocomposite to improve sensor performances especially sensitivity without affecting the mechanical stiffness of the humidity sensitive layer mainly at high moisture level.

CONCLUSIONS

The extraction of cellulose raw material from Tunisian palm date petiole cellulose derivative and synthesis of water soluble CMC (DS = 0.96) under heterogeneous conditions in isopropanol/NaOH reaction medium is firstly presented. Carboxymethylation reaction provided new vibration bands characteristics of carboxyl moieties and reducing in cristallinity. Steric exclusion chromatography showed a classical average molecular weight of 131,000 g mol^{-1}, corresponding to a low viscosity CMC. The viscosity analysis proved the statistic coli conformation and the low viscosity of the prepared CMC. Afterward, a green synthesis method of about 20 nm stabilized-CMC Ag NPs has been reported. Optimal experimental conditions, including $[Ag^+]$ and $[OH^-]$, were determined in order to obtain well-dispersed and long-term stability of quasi-spherical Ag NPs. Finally, Ag-nanocomposite coated quartz microbalance crystal (QCM) was used as sensitive layer for humidity detection. A comparative study showed that the immobilized Ag NPs greatly reduced changes in viscoelastic properties, increased surface area as well as surface local charge density of the CMC, and thus, better stability even at high relative humidity (RH), good reproducibility and linearity (11–98%RH), low hysteresis characteristics, and rapid response and recovery times (14 and 6 s, respectively) were obtained.

ACKNOWLEDGMENTS

The authors are thankful to Pr. Didier Le Cerf for his very helpful assistance in steric exclusion chromatography (SEC) (LPBS, UMR 6270 and FR 3038 CNRS, Université de Rouen, France).

REFERENCES

1. Bruno, P.; Cicala, G.; Corsi, F.; Dragone, A.; Losacco, A. M. *Sens. Actuators B Chem.* **2004**, *100*, 126.
2. Li, Y.; Fan, K.; Ban, H.; Yang, M. *Synth. Met.* **2015**, *199*, 51.
3. Arshak, K.; Moore, E.; Lyons, G. M.; Harris, J.; Clifford, S. A. *Sens. Rev.* **2004**, *24*, 181.
4. Sauerbrey, G. *Z. Phys. A* **1959**, *155*, 206.
5. Üzar, N.; Okur, S.; Arikan, M. *Sens. Actuators A* **2011**, *167*, 188.
6. Hunt, W. D.; Stubbs, D.; Lee, S. H. *Proc. IEEE* **2003**, *91*, 890.
7. Su, P. G.; Kuo, X. R. *Sens. Actuators A* **2014**, *205*, 126.
8. Yao, Y.; Chen, X.; Guo, H.; Wu, Z. *Appl. Surf. Sci.* **2011**, *257*, 7778.
9. Qiu, Y.; Yang, S. *Adv. Funct. Mater.* **2007**, *17*, 1345.
10. Hu, W. L.; Zhou, S. Y.; Liu, L. T.; Ding, B.; Wang, H. P. *Sens. Actuators B* **2011**, *159*, 301.
11. Erol, A.; Okur, S.; Yağmurcukardes, N.; Arikan, M. C. *Sens. Actuators B* **2011**, *152*, 115.
12. Wang, X.; Ding, B.; Yu, J.; Wang, M. *J. Mater. Chem.* **2011**, *21*, 16231.
13. Horzum, N.; Tasçioglu, D.; Okur, S.; Demir, M. M. *Talanta* **2011**, *85*, 1105.
14. Wang, X.; Ding, B.; Yu, J.; Wang, M.; Pan, F. *J. Nanotechnol.* **2010**, *21*, 055502, DOI: 10.1088/0957-4484/21/5/055502.
15. Wang, X.; Zhang, J.; Zhu, Z.; Zhu, J. *Appl. Surf. Sci.* **2007**, *253*, 3168.

16. Su, P. G.; Sun, Y. L.; Lin, C. *Sens. Actuators B* **2006**, *115*, 338.
17. Chen, X. J.; Zhang, J.; Ma, D. F.; Hui, S. C.; Liu, Y. L.; Yao, W. *J. Appl. Polym. Sci.* **2011**, *121*, 1685.
18. Sharma, V. K.; Yngard, R. A.; Lin, Y. *Adv. Colloid Interface Sci.* **2009**, *145*, 83.
19. Lee, K. J.; Nallathamby, P. D.; Browning, L. M.; Osgood, Ch. J.; Xu, X. *Nano Lett.* **2007**, *2*, 133.
20. Roy, B.; Bairi, P.; Nandi, A. *Analyst* **2011**, *136*, 3605.
21. Yongqiang, H.; Guanbo, H.; Zeng, P.; Yue, L.; Qiaojuan, G. *Ch. Yao. J. Gao. Mater. Res. Bull.* **2015**, *70*, 263.
22. Mulfinger, L.; Solomon, S. D.; Bahadory, M.; Jeyarajasingam, A. V.; Rutkowsky, S. A.; Boritz, C. *J. Chem. Educ.* **2007**, *87*, 322.
23. Huynh, K. A.; Chen, K. L. *Environ. Sci. Technol.* **2011**, *45*, 5564.
24. Dehnavi, A. S.; Aroujalian, A.; Raisi, A.; Fazel, S. *J. Appl. Polym. Sci.* **2012**, DOI: 10.1002/app.37594.
25. Sarkar, A.; Kapoor, S.; Mukherjee, T. *J. Phys. Chem. B* **2005**, *109*, 7698.
26. Raveendran, P.; Fu, J.; Wallen, S. L. *J. Am. Chem. Soc.* **2003**, *125*, 13940.
27. Darroudi, M.; Bin Ahmad, M.; Abd, H.; Abdullah, I. *N. Int. J. Nanomed.* **2011**, *6*, 569.
28. Cai, J.; Kimura, S.; Wada, M.; Kuga, S. *Biomacromolecules* **2009**, *10*, 87.
29. Rusli, H.; Gandasasmita, S.; Amran, M. B. *Iran. Polym. J.* **2013**, *22*, 335.
30. Sabitjan, Y.; Inagamov, Gafur, I.; Mukhamedov, J. *Appl. Polym. Sci.* **2011**, *122*, 1749.
31. Chen, X.; Liu, J.; Feng, Z.; Shao, Z. *J. Appl. Polym. Sci.* **2005**, *96*, 1267.
32. Kanipandian, N.; Kannan, S.; Ramesh, R.; Subramanian, P.; Thirumurugan, R. *Mater. Res. Bull.* **2014**, *49*, 494.
33. Wen, J. L.; Sun, Y. C.; Xu, F.; Sun, R. C. *J. Agric. Food. Chem.* **2010**, *58*, 11372.
34. Huggins, M. L. *J. Am. Chem. Soc.* **1942**, *64*, 2716.
35. Mahumd, M. U. *Acta Polym.* **1987**, *38*, 172.
36. Tapio, S.; Daniel, V.; Erkki, P. *Indus. Eng. Chem. Res.* **1994**, *33*, 1454.
37. Sakly, N.; Haj Said, A.; Ben Ouada, H. *Mater. Sci. Semicond. Process.* **2014**, *27*, 130.
38. Aguir, C.; M'Henni, M. F. *J. Appl. Polym. Sci.* **2006**, *99*, 1808.
39. Varshney, V. K.; Gupta, P. K.; Sanjay, N.; Ritu, K.; Amit Bhatt, A.; Soni, P. L. *Carbohydr. Polym.* **2006**, *63*, 40.
40. Zhu, J. J.; Liao, X. H.; Zhao, X. N.; Chen, H. Y. *Mater. Lett.* **2001**, *19*, 91.
41. Shankar, S.; Ahmad, A.; Sastry, M. *Biotechnol. Prog.* **2003**, *19*, 1627.
42. He, S.; Yao, J.; Jiang, P.; Zhang, H.; Xie, S.; Pang, S.; Gao, H. *Langmuir* **2001**, *17*, 1571.
43. Hebeish, A. A.; El-Rafie, M. H.; Abdel-Mohdy, F. A.; Abdel-Halim, E. S.; Emam, H. E. *Carbohydr. Polym.* **2010**, *82*, 933.
44. Xie, J.; Wang, H.; Lin, Y.; Zhou, Y.; Wu, Y. *Ceram. Int.* **2013**, *39*, 3621.
45. Arai, H.; Seiyama, T.; Gopel, W.; Hesse, J.; Zemel, J. N. *Sens. A* **1992**, *3*, 981.